

The displacement energies of cations in perovskite (CaTiO₃)

Katherine L. Smith^{a,*}, Nestor J. Zaluzec^b

^a *Materials and Engineering Science, Australian Nuclear Science and Technology Organisation, P.M.B. 1, Menai, NSW 2234, Australia*

^b *Materials Science Division, Argonne National Laboratory, 9700 North Cass Ave, Argonne, IL 60439, USA*

Received 8 June 2004; accepted 29 September 2004

Abstract

High angular resolution electron channelling X-ray spectroscopy (HARECXs) was used to monitor the intensity ratio of CaK α /TiK α X-rays emitted by perovskite (CaTiO₃) as a function of incident electron beam orientation. The collected HARECXs data suggest that the displacement energies of calcium and titanium in perovskite (CaTiO₃) are 82 ± 11 eV and 69 ± 9 eV, respectively. These values are approximately 40% larger than those currently used to convert ion doses applied to oxides into dpa using SRIM.

© 2004 Elsevier B.V. All rights reserved.

PACS: 61.82.Fk; 61.85.+p

1. Introduction

Radiation damage can affect the chemical durability of phases and/or assemblages (waste forms) designed to host high level radioactive waste (HLW) [1]. As HLW waste forms are designed to hold actinides for geologic periods of time (10^4 – 10^6 years), it is desirable to be able to predict and/or model the occurrence of radiation damage induced defects over long time periods. Data to aid the development of models can be collected from (a) natural analogue minerals or from (b) experiments where waste forms are doped with short-lived actinides or irradiated with high-energy heavy ions or fast neutrons [2]. To compare data from these experiments, it is necessary to convert the various disparate dose units into the standard unit of displacements per

atom (dpa). Knowledge of the displacement energies (E_d values) of the ions in the actinide host phases is essential for these calculations.

High angular resolution electron channelling X-ray spectroscopy (HARECXs) is a transmission electron microscope (TEM) based technique which exploits electron channelling phenomena [3–10]. It was originally developed to determine crystallographic site occupancies in fully crystalline matrices but has been used to monitor the onset of radiation damage induced cation mixing in spinel [11]. HARECXs measurements involve rocking the incident electron beam under computer control along specific crystallographic axes and simultaneously monitoring the resulting characteristic X-ray emission signal as a function of orientation of the beam to the crystal. The relative intensities of characteristic peaks change as a function of channelling along crystallographic directions and alter in response to local composition and/or changes in the perfection of the crystal. This phenomenon is particularly useful when applied to directions in the crystalline lattices which present

* Corresponding author. Tel.: +61 (0)2 9717 3505; fax: +61 (0)2 9543 7179.

E-mail address: kls@ansto.gov.au (K.L. Smith).

ordered distributions of different atomic species on adjacent lattice planes.

Perovskite (CaTiO_3 , $Pcmm$, $a = 0.53829$, $b = 0.76453$, $c = 0.54458$ nm [12]) has been proposed as an actinide host phase in various titanate ceramic waste forms for high level radioactive waste [2,13]. Fully crystalline perovskite is comprised of alternate planes of (i) titanium and oxygen and (ii) calcium ions parallel to (101) and consequently shows strong ordering effects in electron channelling at this orientation.

In this investigation, areas of selected grains in TEM specimens were irradiated with high-energy electrons using the HVEM-Tandem User Facility (HVEM-Tandem) at Argonne National Laboratory. Then HARECXs measurements were taken from both non-irradiated and irradiated parts of the grain. From these data, the threshold for cation radiation damage was estimated, the identity of displaced ions was established, and the displacement energies of Ca and Ti were calculated.

2. Experimental procedure

Areas of two or more perovskite grains in TEM specimens were irradiated with 0.62 MeV, 0.75 MeV or 0.9 MeV electrons using the HVEM-Tandem to fluences of 2×10^{23} e/cm². Previous authors witnessed radiation damage effects in oxides ($\alpha\text{-Al}_2\text{O}_3$ [14], ZnO [15], MgO [16]) irradiated with electrons of 0.1–0.3 MeV to fluences of between 3.4×10^{21} and 5.3×10^{22} e/cm² (5.3×10^{22} , 6×10^{21} e/cm² and 3.4×10^{21} e/cm², respectively). We chose to irradiate specimens to fluences of 2×10^{23} e/cm² as this is towards the upper end of the range used by previous authors and could be accomplished in a reasonable time period (≈ 3 h) using the HVEM.

After irradiation, the samples were transferred to the analytical microscope, and the irradiated grains were oriented so that their electron diffraction patterns contained only the $\langle 101 \rangle$ systematic row of reflections, and HARECXs measurements were recorded from both non-irradiated and irradiated parts of the grains.

All HARECXs data were measured on a Philips EM 420T analytical TEM fitted with an EDAX UTW Si(Li) detector (FWHM of ≈ 150 eV at Mn K α). Nominal probe sizes were 200–500 nm. Individual grains were oriented so that a single row of systematic reflections (e.g. $\langle 101 \rangle$) was present in their selected area diffraction pattern. The direction of the incident electron probe was then systematically tilted along the plane normal direction (e.g. [101]) via direct computer control of the beam tilt coils. The resulting HARECXs data (X-ray spectra as a function of tilt) were recorded using customised computer programs running on an EDAX 9900 micro-analyser system. As experimental conditions were set with the TEM in diffraction mode, tilt angles are given

here in units of reciprocal nanometers (1/nm). Typical acquisition times ranged from 1 to 5 h. Essential to the success of these measurements was the stability of the probe current, minimal specimen drift and absence of hydrocarbon contamination.

There are a number of factors that affect the absolute X-ray intensities emitted by TEM specimens. Among these factors are X-ray absorption, specimen preparation, hydrocarbon contamination during electron irradiation or illumination and operating conditions (accelerating voltage, detector efficiency, etc.). The details of such issues do not generally bear on the arguments given here. We present in this paper comparisons of ratios of X-ray peaks in arbitrary units rather than absolute values, in order to diminish the number and effect of specimen and operating dependent variables.

3. Results

Fig. 1 shows plots of three data sets of the Ca K/Ti K X-ray intensity ratios from one grain, part of which was irradiated with 0.75 MeV electrons. One data set was collected by tilting the incident beam away from (121), towards the [121] plane normal. The structure of perovskite is not differentiated along (121), that is the structure has no preponderance of any one elemental species along any selected direction in any projected plane. Consequently, the experimental intensity ratio

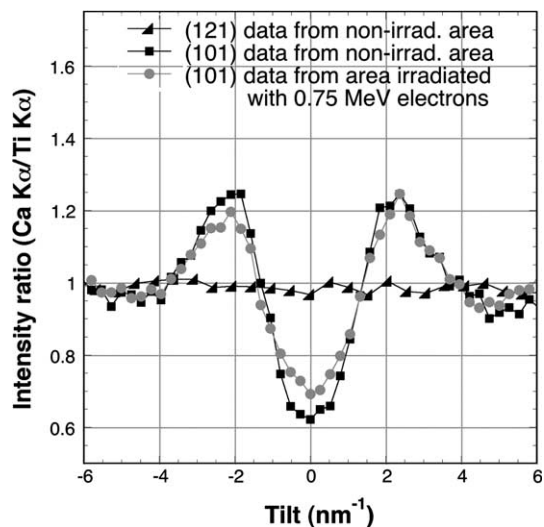


Fig. 1. Plots of the Ca K/Ti K X-ray emission ratio from different areas of single perovskite grain as a function tilt along the (121) and (101) rows of systematic reflections in reciprocal space. The data points designated by circles came from an area of the grain that had previously been irradiated with 0.75 MeV electrons.

of Ca/Ti should be approximately independent of orientation. The observed variation is nominally constant and therefore indicates the typical experimental scatter in the measurements. The two remaining data sets in Fig. 1 were collected from non-irradiated and irradiated areas of the same grain by tilting the incident beam away from (101), towards the [101] plane normal. In this direction, one will observe an orientation dependence of the Ca/Ti ratio since there is a partitioning of Ca and Ti along this direction in the crystal lattice. Although we clearly observe an orientation dependence along [101] and not along [121], it is significant to note that within experimental error there are no significant differences between the irradiated and non-irradiated areas. This indicates that the elemental distribution between these areas is essentially identical. All these data are representative of the results from grains irradiated with 0.75 MeV electrons.

Figs. 2 and 3 show plots of the Ca K/Ti K shell X-ray intensity ratio as a function of orientation as the incident electron beam was tilted away from a particular family of planes as described above. Data in each figure were taken from regions of individual grains irradiated with 0.62 or 0.90 MeV electrons, respectively, and are also representative of the results from all measurements.

Using the non-ordered channelling data as a measure of our experimental error, we see that there is no significant difference between the HARECX data collected from non-irradiated and irradiated areas of the same grain previously bombarded with 0.75 MeV or

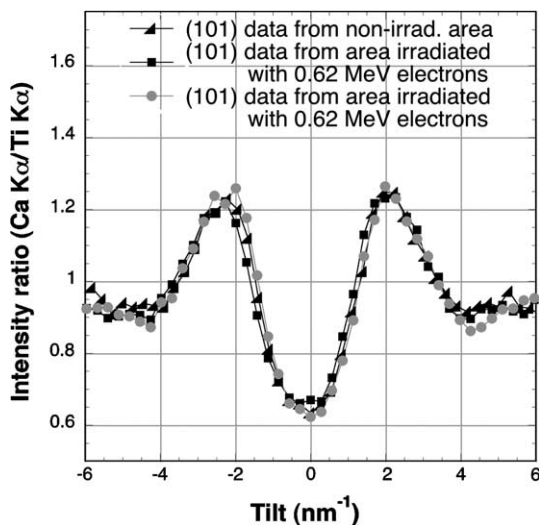


Fig. 2. Plots of the Ca K/Ti K X-ray emission ratio from different areas of perovskite grain as a function tilt along the (101) row of systematic reflections in reciprocal space. The data points designated by circles and triangles came from an area of the grain that had previously been irradiated with 0.62 MeV electrons.

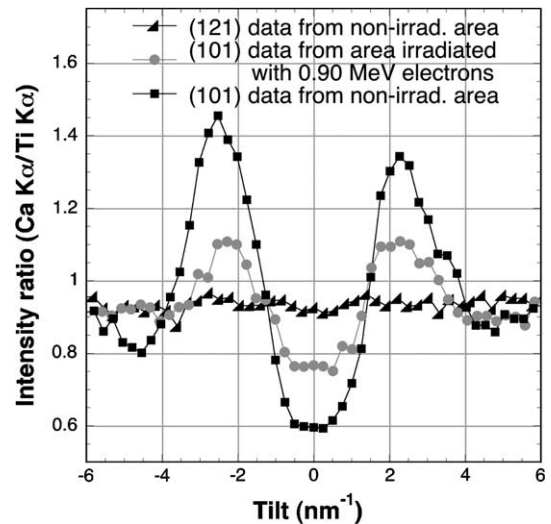


Fig. 3. Plots of the Ca K/Ti K X-ray emission ratio from different areas of perovskite grain as a function tilt along the (121) and (101) rows of systematic reflections in reciprocal space. The data points designated by circles came from an area of the grain that had previously been irradiated with 0.90 MeV electrons.

0.62 MeV electrons (Figs. 1 and 2, respectively). However, there is a substantial difference between the data collected from the non-irradiated areas and the 0.90 MeV electron irradiated areas of grains (Fig. 3).

The fact that in Figs. 1 and 2, the Ca K/Ti K ratio of adjacent non-irradiated and irradiated areas are identical within experimental error, indicates that electrons with energies of less than 0.75 MeV do not cause cationic rearrangement in perovskite. In contrast, Fig. 3 shows that 0.90 MeV electrons do produce cationic rearrangement as witnessed by the change in the Ca K/Ti K ratio between non-irradiated and irradiated zones. In concert, Figs. 1–3 show that high-energy electrons cause elemental disorder (radiation damage) in perovskite and that the threshold for damage lies between 0.75 and 0.90 MeV.

4. Discussion

4.1. Is the damage threshold indicated by HARECX data due to anion or cation displacement?

Previous authors, Cooper et al. [17], studied CaTiO₃ perovskite using time-resolved cathodoluminescence (CL) spectroscopy and found that there was a threshold for optical emission at an incident electron energy of 0.26 ± 0.02 MeV. For relativistic particles such as electrons, the maximum energy T_m (eV) transferable from an incident electron of energy E (MeV) to a lattice ion of mass number A is given by [18]:

$$T_m = 2147.7E(E + 1.022)/A. \quad (1)$$

On the basis of their observations, Eq. (1) and the results of previous authors, Cooper et al. concluded that incident 0.26 MeV electrons were sufficiently energetic to displace oxygen ions in perovskite for periods of several microseconds and that the displacement energy of oxygen in perovskite was 45 ± 4 eV. The HARECXS data in this study however show a damage threshold between incident electron energies of 0.75 MeV and 0.90 MeV. Consequently the threshold indicated by our HARECXS data presumably represents the onset of cation displacement.

4.2. Which cation species is being displaced?

To determine if the threshold for cation displacement between 0.75 MeV and 0.90 MeV is related to the displacement of Ca or Ti or both cations, we closely examined data collected from grains that had been partly irradiated with 0.90 MeV electrons. Spectra were collected from approximately 10 points on single grains: some of the spectra were taken from non-irradiated areas and some were taken from irradiated areas. Comparison of raw Ca and Ti spectra from non-irradiated and irradiated parts of the same grains irradiated with 0.90 MeV electrons suggests that both Ca and Ti atoms are displaced. However, ion damage induced during specimen preparation and/or thickness effects can affect spectra. Consequently we decided to normalise the data from single grains to eliminate any specimen preparation and thickness effects.

Figs. 4 and 5 show normalised Ca ratios and Ti ratios, respectively, as a function of orientation and are representative of data from various grains. The plots labelled (a) and (b) in Figs. 4 and 5 were calculated as follows.

- (a) The normalised ratio of the same K shell X-ray intensity at two points in the non-irradiated area of a grain (calculated according to Eq. (2) below) as a function of orientation. The nominal orientation dependence of this plot should be approximately horizontal and such a plot indicates the amount of experimental scatter of our measurements. The normalisation, discussed below, was selected to effectively remove specimen preparation and thickness effects from appearing on the graph and complicating the interpretation.
- (b) The normalised ratio of the same K shell X-ray intensity at a point in the irradiated area of a grain versus the same K shell X-ray intensity at a point in the non-irradiated area of the same grain (calculated according to Eq. (2) below) as function of orientation. Again the data were normalised to remove any specimen preparation and thickness effects,

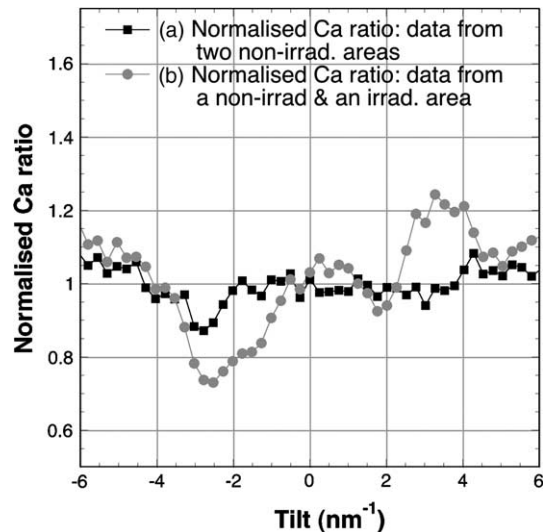


Fig. 4. (a) The normalised ratio of the CaK shell X-ray intensity at two points in the non-irradiated area of a grain (calculated according to Eq. (2)) as function of orientation. This plot indicates the amount of experimental scatter. (b) The normalised ratio of the CaK shell X-ray intensity at a point in the irradiated area of a grain versus the CaK shell X-ray intensity at a point in the non-irradiated area of the same grain (calculated according to Eq. (2)) as function of orientation. This plot indicates that there is change in the elemental distribution of Ca between the irradiated and non-irradiated zones.

and thus any difference in this plot 'b' relative to plot 'a', indicates that there is a change in the elemental distribution of that particular element between the irradiated and non-irradiated zones.

The plotted value, x , at each orientation was calculated as follows:

$$x = \frac{(K\alpha(1)/\sqrt{[K\alpha(1)]})}{(K\alpha(2)/\sqrt{[K\alpha(2)]}}, \quad (2)$$

where $K\alpha(1)$ is the intensity of the $K\alpha$ X-ray peak of a particular element (e.g. Ca) from one area of the specimen at a particular orientation and $K\alpha(2)$ is the intensity of the $K\alpha$ X-ray peak of the same element (e.g. Ca) from a second area of the specimen at the same orientation.

This simple normalisation effectively removes the variation due to thickness changes in the two measurement points, but does not remove any orientation dependent effects. Fig. 4 shows the results of this comparison for Ca, while Fig. 5 shows equivalent plots of Ti data.

Inspection of Fig. 4 shows that the variation in the ratio of normalised Ca X-ray data from irradiated and non-irradiated areas is about two times greater than experimental scatter, as indicated by the variation in

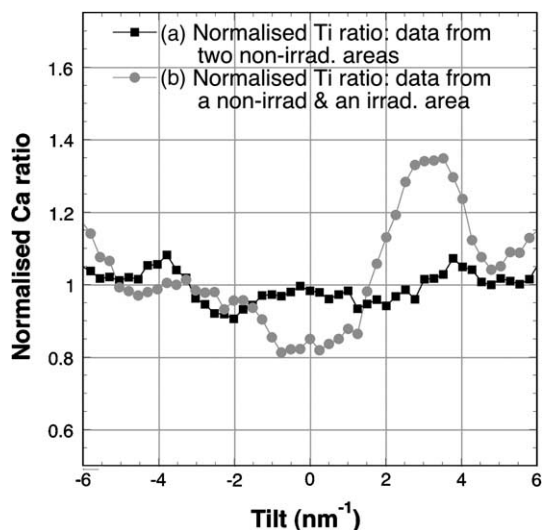


Fig. 5. (a) The normalised ratio of the TiK shell X-ray intensity at two points in the non-irradiated area of a grain (calculated according to Eq. (2)) as function of orientation. This plot indicates the amount of experimental scatter. (b) The normalised ratio of the TiK shell X-ray intensity at a point in the irradiated area of a grain versus the TiK shell X-ray intensity at a point in the non-irradiated area of the same grain (calculated according to Eq. (2)) as function of orientation. This plot indicates that there is change in the elemental distribution of Ti between the irradiated and non-irradiated zones.

the ratio of data from two non-irradiated areas. Likewise, Fig. 5 shows that the variation in the ratio of normalised Ti X-ray data from irradiated and non-irradiated areas is about three times greater than experimental scatter, as indicated by the variation in the ratio of data from two non-irradiated areas. This demonstrates that there is a change in the elemental distribution between irradiated and non-irradiated areas for both Ca and Ti and shows that the energy transmitted by 0.90 MeV electrons to the cations in perovskite displaces both Ca and Ti cations.

4.3. The displacement energies of calcium and titanium in perovskite: calculations thereof and comments on usage

Table 1 shows the maximum energy transferable to Ca and Ti ions by electrons with energies of 0.62, 0.75 and 0.90 MeV, calculated on the basis of Eq. (1). The datum for oxygen displacement is included for comparison and completeness.

The data collected and analysis undertaken in this study show that:

- the energy input to perovskite cations by 0.75 MeV electrons must be below the displacement energies of both of Ca and Ti and

Table 1
Maximum energies transferable (T_m) from high-energy electrons to atomic species in crystalline perovskite

	T_m to calcium (eV)	T_m to titanium (eV)	T_m to oxygen (eV)
0.26 MeV	18	15	45
0.62 MeV	55	46	137
0.75 MeV	71	60	178
0.90 MeV	93	78	232

- the energy input to perovskite cations by 0.90 MeV electrons is above the displacement energies of both of Ca and Ti.

Thus the findings of this study indicate that the displacement energies of calcium and titanium ions in perovskite are 82 ± 11 eV and 69 ± 9 eV, respectively.

As mentioned earlier, data for input into the structural modelling of the radiation damage response of actinide-bearing waste forms over geologic time can be collected by examining natural samples, or from experiments where waste forms are doped with short-lived actinides or irradiated with high-energy heavy ions or irradiated with fast neutrons; and comparison of data from different experiments necessitates conversion of various dose units into the standard unit of displacements per atom (dpa). Data are most commonly collected from experiments wherein synthetic samples are irradiated with high-energy heavy ions as these experiments are the most easily accomplished and do not produce radioactive products. In order to convert doses of ions per unit area into dpa,

- the program SRIM [19] is used to calculate the number of displacements per ion as a function of specimen depth,
- the average of this curve is calculated,
- then the average is multiplied by the ion dose (in units of ions per unit area) and divided by the number of atoms per unit volume.

SRIM requires various input parameters including chemical formula of the target material, its density, the displacement energies of the ions in the target material and their binding energies.

In recent ion irradiation studies of perovskites (ABO_3 , where A and B are cations) and pyrochlores ($A_2B_2O_7$, where A and B are cations), various authors have used 50 eV as the displacement energy of both anions and cations in their specimens [20–23]. It is likely that 50 eV is a valid estimate for the displacement energy of oxygen in most perovskites and pyrochlores, as time-resolved cathodoluminescence experiments have shown that the displacement energies of oxygen in some

titanate and zirconate perovskites and pyrochlores are $\approx 50 \pm 5$ eV [24]. However, the results of this study suggest that the displacement energies of the cations in CaTiO_3 , and therefore possibly other perovskites and oxides, are at least 69 eV, that is approximately 40% larger than those recently used to convert ion doses applied to oxides into dpa using SRIM.

In order to facilitate comparison of data from different authors and to assist the recalculation/correction of radiation damage doses, it is our opinion that ion irradiation doses should be published in units of ions/cm² (or equivalent) as well as in units of dpa, until all the displacement energies and binding energies of a particular specimen have been unequivocally established.

4.4. Could the displacement of one species of cation in combination with the displacement of oxygen cause the displacement of the second species of cation?

We consider it unlikely that displacement of one species of cation in combination with the displacement of oxygen would necessarily result in the displacement of the second species of cation, as the work of previous authors shows that oxygen vacancies in perovskite are unlikely to persist at room temperature. Specifically, Weber et al. [25] saw significant annealing of temporary oxygen vacancies in SrTiO_3 at temperatures between 200 and 400 K. Cooper et al. [17] found that (a) CL emission from perovskite only continued for a few microseconds after electron irradiation and (b) the shape and intensity of the spectra did not depend on the order in which data was taken. That is, Cooper et al. could irradiate their sample with electrons of low energy (e.g. 0.2 MeV) after irradiating with electrons of high energy (up to 0.6 MeV) and get the same CL spectra.

If one wanted to prove that different incident electron energies were needed to displace calcium and titanium, one would need to irradiate specimens with energies intermediate between 0.75 and 0.9 MeV and conduct additional HARECXs experiments.

5. Conclusions

HARECXs data suggest that the displacement energies of calcium and titanium ions in perovskite are 82 ± 11 eV and/or 69 ± 9 eV, respectively. These values are approximately 40% larger than those currently used to convert ion doses applied to oxides into dpa using SRIM.

Acknowledgments

The authors thank the HVEM-Tandem User Facility staff at Argonne National Laboratory for assistance dur-

ing electron irradiations, particularly Charlie Allen, Ed Ryan, Stan Ockers, Tony McCormick, Pete Baldo and Lauren Funk. The facility is supported by the US DOE Basic Energy Sciences, under contract W-31-109-ENG-38. The authors also thank Gregory R. Lumpkin of the University of Cambridge, UK for constructive review and Lou (E.R.) Vance of ANSTO for providing the perovskite sample.

References

- [1] R.A. Van Konynenburg, Lawrence Livermore National Laboratory, Report Number UCRL ID 128580, 1997, p. 31.
- [2] R.C. Ewing, W.J. Weber, F.W. Clinard, *Progr. Nucl. Energy* 29 (1995) 63.
- [3] P. Duncumb, *Philos. Mag.* 7 (1962) 2101.
- [4] J. Cowley, *Acta Crystallogr.* 17 (1964) 33.
- [5] J. Spence, J. Taftø, *J. Microsc.* 130 (1983) 147.
- [6] I. Anderson, *Acta Mater.* 45 (1997) 3897.
- [7] L.J. Allen, T.W. Josefsson, C.J. Roossouw, *Ultramicroscopy* 55 (1994) 258.
- [8] N.J. Zaluzec, *Microsc. Microanal.* 5 (Suppl. 2) (1999) 712.
- [9] N.J. Zaluzec, *Microsc. Microanal.* 6 (Suppl. 2) (2000) 938.
- [10] N.J. Zaluzec, K.L. Smith, *Microsc. Microanal.* 7 (Suppl. 2) (2001) 354.
- [11] T. Soeda, S. Matsumura, C. Kinoshita, N.J. Zaluzec, *J. Nucl. Mater.* 283–287 (2000) 952.
- [12] C.J. Rossouw, P.S. Turner, T.J. White, *Philos. Mag.* 57 (1988) 209.
- [13] G.R. Lumpkin, *J. Nucl. Mater.* 289 (2000) 136.
- [14] G. Das, *J. Mater. Sci. Lett.* 2 (1983) 453.
- [15] T. Yoshie, *Philos. Mag.* 40 (1979) 297.
- [16] J.V. Sharp, D. Rumsby, *Radiat. Eff.* 17 (1973) 65.
- [17] R. Cooper, K.L. Smith, M. Colella, E.R. Vance, *J. Nucl. Mater.* 289 (2000) 199.
- [18] E. Sonder, W.A. Sibley, in: J.H. Crawford Jr., L.M. Slifkin (Eds.), *Point Defects in Solids*, vol. I, Plenum, New York, 1972, p. 201.
- [19] J. Ziegler, J.P. Biersack, U. Littmark, *The Stopping Range of Ions in Solids*, Pergamon, New York, 1985.
- [20] A. Meldrum, L.A. Boatner, W.J. Weber, R.C. Ewing, *J. Nucl. Mater.* 300 (2002) 242.
- [21] A. Meldrum, L.A. Boatner, R.C. Ewing, *Nucl. Instrum. and Meth. B* 207 (2003) 28.
- [22] J. Lian, X.T. Zu, K.V.G. Kutty, J. Chen, L.M. Wang, R.C. Ewing, *Phys. Rev. B* 66 (2002) 054108.
- [23] J. Lian, L. Wang, J. Chen, K. Sun, R.C. Ewing, J.M. Farmer, L.A. Boatner, *Acta Mater.* 51 (2003) 1493.
- [24] K.L. Smith, M. Colella, R. Cooper, E.R. Vance, *J. Nucl. Mater.* 321 (2000) 19.
- [25] W.J. Weber, W. Jiang, S. Thevuthasan, R.E. Williford, A. Meldrum, L.A. Boatner, in: G. Borstel, A. Kruminis, D. Miller (Eds.), *Defects and Surface-induced Effects in Advanced Perovskites*, Kluwer Academic, The Netherlands, 2000, p. 317.